



25<sup>th</sup> ABCM International Congress of Mechanical Engineering  
October 20-25, 2019, Uberlândia, MG, Brazil

## COB-2019-0275

# FATIGUE FRACTURE ANALYSIS IN DRIVE SHAFTS OF CHIPPING AND REFINING MACHINES IN A CELLULOSE PULP AND PAPER PLANT

**Alexandre Nakayama**

Klabin S.A. unidade Monte Alegre, Telêmaco Borba, Paraná, Brazil  
nakayama@klabin.com.br

**Abstract.** *Fatigue failure is one of the most common and critical in mechanical components and structure, therefore its study and understanding is of vital importance for the design, operation and maintenance of industrial systems. In the cellulose pulp and paper industry, wood chipping and pulp refining are essential processes to ensure final product quality and plant productivity with equipments experimenting high loads cycles, intermittent impacts and input fluctuations. In this paper, two drive shafts, one from a wood chipper and one from a refiner that failed during operation were analyzed with focus on fracture surface interpretation in order to understand the causes and damage mechanism. The methods used to analyze the fracture surface were macro and micro fractography with complementary tests of material chemical analysis, metallographic analysis and mechanical test. It was concluded that the failure mechanism was fatigue with cracks initiation in stress concentration points closely related to surface finishing.*

**Keywords:** *fatigue, fractography, fracture characterization.*

## 1. INTRODUCTION

In 2018, Brazil was the second largest cellulose pulp and the eighth largest paper producing country in the world with an annual production of 21.1 and 10.4 million metric tons respectively. Pulp and paper industry generated in that year approximately US\$ 10.74 billion representing 10.6 % of total Brazilian exports (IBA, 2019). In order to keep the international competitiveness, it is vital to pulp and paper mills to increase productivity and reduce costs. As a continuous production process, equipments maintenance downtimes represent one of the largest costs and losses to mills operations. Therefore, the understanding of failure mechanisms the equipments are subjected plays essential role in reliability increase, besides increasing the mills operations safety.

Rotating equipments are numerous in the cellulose pulp and paper productions, such as pumps, compressors, gear boxes and fans. Among the most critical rotating equipments are wood chippers and pulp refiners due to the severity of service. A common damage mechanism in these rotating equipments is fatigue that is defined as a progressive, localized and permanent structural alteration that occurs in components under repeated or fluctuating loads and deformations generally less than the yield strength figure in static loads for the material that can lead to a crack or a complete failure after a certain number of fluctuation cycles (ASTM E1823, 1996).

The understanding of fatigue damage mechanism is essential for the evaluation of the numerous conditions that affect the fatigue-life such as: surface finishing, residual stresses and environment influence. This understanding can contribute greatly to development of predictive maintenance methods (Sodré, 2008).

In this context, this paper investigates through fracture characterization two drives shafts that failed due to fatigue mechanism. One shaft was from a wood chipper responsible to cut wood logs into small fragments for the cooking in the digester and the other shaft was from a refiner responsible to milling the cellulose fibers after cooking to enable an adequate paper sheet formation.

## 2. MATERIALS AND METHODS

The fractured shafts were preserved and sampled for the failure analysis. Since the interpretation of fracture surface is an essential procedure of failure analysis (Ihara, 2018), the methods used to investigate were fractography in macro and micro scale in order to search for characteristics related to energy absorption and tolerance to plastic deformation. According to Oliveira (2017), the fracture surface presents a topography that is a result from failure mechanisms actuation and holds the whole historical stages of the process. Informations gathered from a fracture surface analysis are crucial in order to evaluate the failure root causes and the factors that influenced it and may be used to prevent future similar failures.

Fractography is a method to analyze a fracture surface to determine the causes taking into account failure initiation point, propagation mode, material structure and composition. It identifies fracture aspects and establishes relations of

presence or absence of these aspects with the sequence of events that led to the component failure (Ihara, 2018). Macro scale fractography is a visual examination to identify fracture initiation sites, material imperfections, presence of surface coatings, corrosion and other structural details that contribute to failure besides identify areas of the surface where more informations on the failure mechanism can be gathered through more detailed and microscopic analysis (Zipp and Dahlberg, 1987). The fracture surfaces macrofractography of both shafts was performed to characterize the general conditions to subsequently define the microfractography strategy.

Micro scale fractography was performed with optical microscope Olympus BX60M in the surface near the crack initiation region for both shafts. Samples for microfractography were mounted in Bakelite polymeric material holders and sanded with sand grades in the decreasing roughness order: 220, 320, 400, 600, 1000, 1200, 1500 and 2000. During the sanding process, samples were rotated in each change of sandpaper grade to overlap perpendicularly the orientation marks of the previous sandpaper in order to keep the maximum surface flatness and improve the optical microscope imaging.

After sanding process, samples were polished in three stages with alumina with particles size 1  $\mu\text{m}$ , 0.3  $\mu\text{m}$ , and 0.1  $\mu\text{m}$  in this sequence followed by washing process with ethyl alcohol and dried with cold air blast to remove any remainder fragment from the surface to be analyzed. Samples surfaces were chemically etched with Nital, a solution of nitric and ethyl alcohol in a 2.0 % volume proportion. This chemical etching reveals the grain boundaries and allows the measurement of grain sizes and identification of morphology and microstructure constituents. According to Voort (2001), Nital is the most used chemical etchant for steel analysis and is excellent for revealing martensite structures, ferrite in martensitic matrix and ferrite grain boundaries in low carbon steels.

This paper method followed similarly to Godefroid et al. (2015) involving the stages: use evaluation of the components in the equipment, sampling and preparation of the fractured surfaces, macro and micro fractography, metallographic analysis, chemical analysis and hardness test for both shafts.

### 3. RESULTS AND DISCUSSION

#### 3.1 Refiner shaft

The fractured shaft was the drive component of a cellulose fiber refiner whose main objective is to mill the fiber in order to adjust its physical-mechanical characteristics such as length and flexibility to provide the requested quality of the paper (Barbosa, 2015). The refiner consists of a rotating rotor and a stator both equipped with bladed tools in the form of a segmented disc that impose mechanical forces in the cellulose fiber. The refining is a high energy demanding process, approximately 150 to 250 kWh/fiber ton that requires sturdy equipments to withstand the stresses involved. Figure 1 shows the refiner unit installation and the drive shaft position.



Figure 1. Refiner installation with indication of drive shaft

##### 3.1.1 Macrofractography analysis

Figure 2 presents the fracture general aspect. Crack initiation is located at the bottom of the keyseat with “beach marks” in curved shape and partially concentric to crack initiation point. The region near the line of the keyseat bottom reflects more intensively the light. The region opposed to the keyseat indicated as crack propagation final region presents a bright surface marking a brittle fracture as a result of unstable crack propagation.

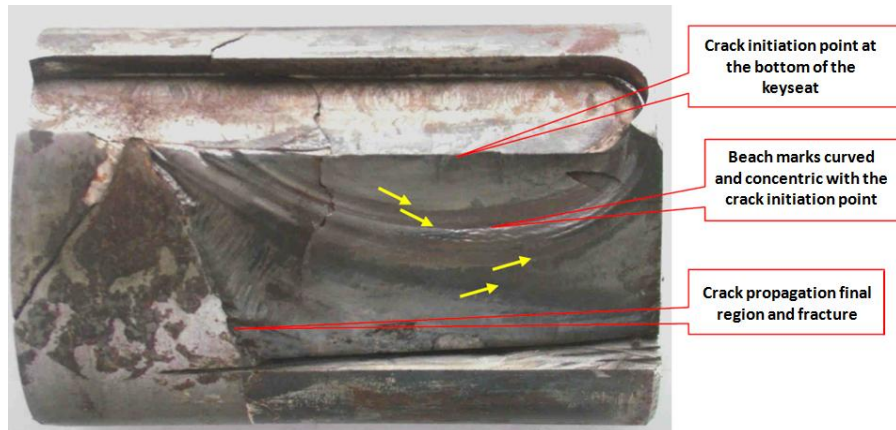


Figure 2. Shaft fracture surface

### 3.1.2 Chemical analysis

Sample from the shaft was submitted to chemical analysis by optical emission spectrometry method with reference to ASTM E415:2015 (Spectroscan, 2018). The sample composition is similar to the expected material SAE 4140 but with a C content slightly higher than specified by SAE norm. Content, in % weight, of C, Si, Cr, Mo, Mn, S and P of the sample analyzed and the standard SAE 4140 composition are shown in Tab. 1. The shaft sample is a hypoeutectoid microalloyed steel.

Table 1. Chemical composition in % weight of shaft sample and SAE 4140

|                     | C           | Si          | Cr          | Mo          | Mn          | S                    | P                    |
|---------------------|-------------|-------------|-------------|-------------|-------------|----------------------|----------------------|
| <b>Shaft Sample</b> | 0,468       | 0,276       | 1,009       | 0,161       | 0,725       | 0,004                | 0,005                |
| <b>SAE 4140</b>     | 0,37 - 0,44 | 0,15 - 0,35 | 0,75 - 1,20 | 0,15 - 0,25 | 0,65 - 1,10 | 0,030 <sub>max</sub> | 0,040 <sub>max</sub> |

### 3.1.3 Metallographic analysis

A surface for metallographic analysis was selected in the area of crack nucleation. A sample was taken, prepared and etched (Nital 2%) for microscopic investigation. Figure 3 presents the microstructure constituted of tempered martensite matrix.

From the microscopic investigation of the failure surface it is possible to confirm the fatigue as the main mechanism leading to crack nucleation and stable growth. The fracture surface has a mainly flat surface without plastic deformation in the load direction, that is, at the torque direction to rotate de shaft, and presents beach marks. It also presents a region of transition from stable to unstable crack growth and the final fracture with typical characteristics of brittle fracture.

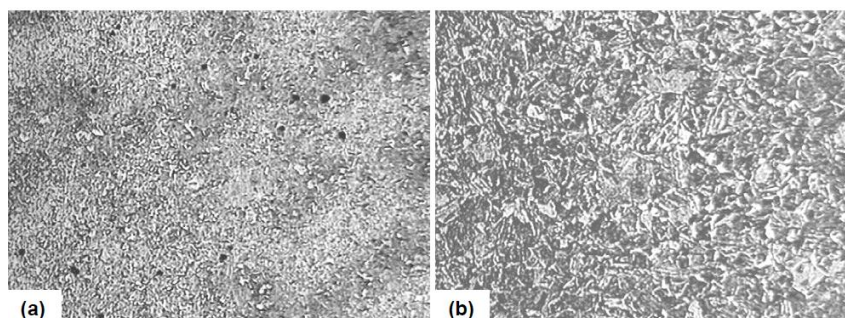


Figure 3. Microstructure of tempered martensite matrix (a) Nital 2%, 100x (b) Nital 2%, 400x

Figure 4 presents a micrographic image from a region at the bottom of the keyseat with nucleation of micro cracks. These cracks are nucleating in a high stress concentration point of the shaft at stage I of fatigue cracking as indicated at Fig. 5.

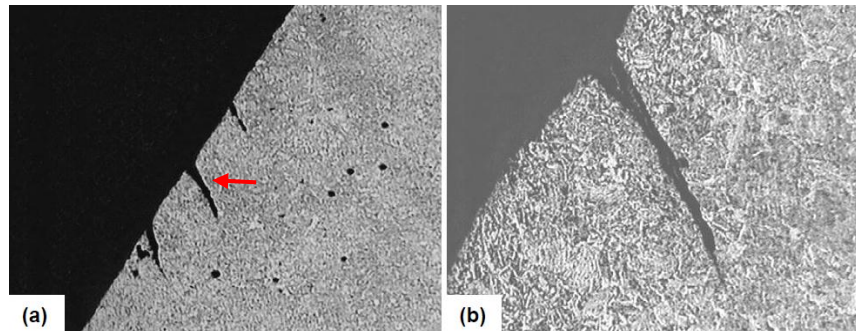


Figure 4. Micro cracks nucleating at the bottom edge of the key seat and a detail from the indicated transgranular crack  
 (a) Nital 2%, 100x (b) Nital 2%, 400x

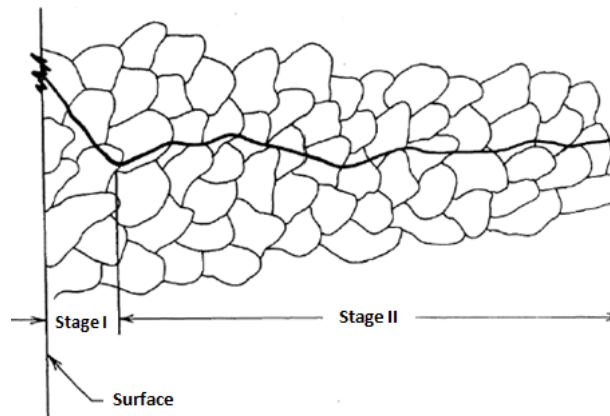


Figure 5. Schematic drawing of transgranular fatigue crack with Stage I and II of fatigue (adapted from Ihara, 2018)

### 3.1.4 Mechanical test

The sample used for the metallographic analysis was firstly submitted to hardness testing with 0.10 mm, 0.50 mm and 1 mm depth from the shaft surface. Hardness measurements in HV and then converted to HRC are as expected related to material specification. Table 2 and 3 show the hardness measurement results and standard data for SAE 4140.

Table 2. Hardness measurement of the shaft sample in three levels from the surface

|              | Surface Depth (mm) | Hardness (HRC) |
|--------------|--------------------|----------------|
| Shaft Sample | 0,1                | 32             |
|              | 0,5                | 32             |
|              | 1                  | 30             |

Table 3. Hardness of the standard SAE 4140 tempered in two temperatures after quenched in oil from 845 °C

|          | Tempering temperature (°C) | Hardness (HRC) |
|----------|----------------------------|----------------|
| SAE 4140 | 540                        | 37             |
|          | 595                        | 33             |

### 3.2 Wood chipper shaft

The fractured shaft was the drive component of a disc wood chipper that consists of a rotating rotor with cutting knives and a feed plate with an anvil that supports the wood log. Chipping is intensive in energy demand and the equipment experiments high intermittent loads due to logs feeding and diameters variation. Figure 6 shows the position of the chipper drive shaft and the drive pulley.

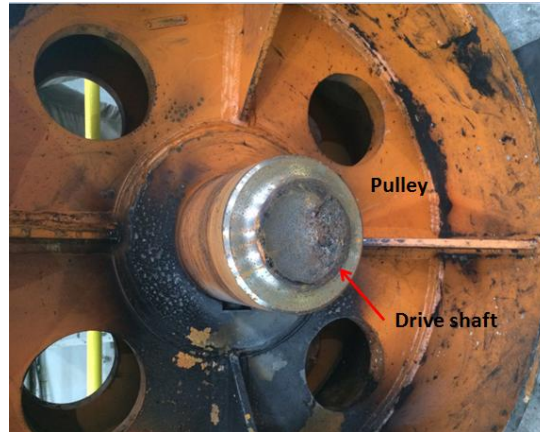


Figure 6. Wood chipper pulley and of drive shaft installation

### 3.2.1 Macrofractography analysis

Figure 7 presents the fracture general aspect. Crack initiation is located at the interface of the shaft base material with the thin layer of coating. The region of crack propagation reflects more intensely the light. The surface presents “beach marks” around the shaft axis with direction opposite to the shaft rotation.

The region around the shaft center presents a smoother surface due to rubbing contact between the two parts of the shaft after the fracture. Pulley side section was decelerating and the motor side section was still rotating with drive rotation.

Through surface macro analysis taking into account light reflectiveness and apparent roughness it is possible to identify the crack initiation point, the region where the crack propagated in a stable way, the crack propagation final region and the brittle like final fracture.

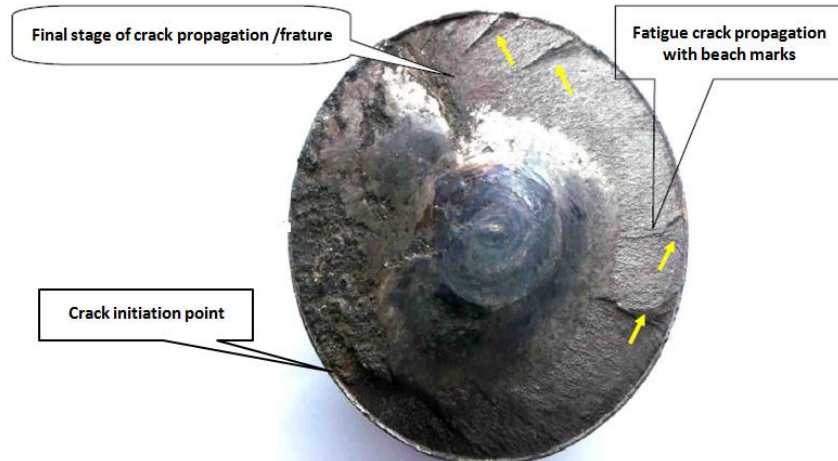


Figure 7. Shaft fracture surface

### 3.2.2 Chemical analysis

Sample from the shaft was submitted to chemical analysis by optical emission spectrometry method with reference to ASTM E415:2015 (Spectroscan, 2019). The sample composition is similar to the expected material SAE 4140. Content, in % weight, of C, Si, Cr, Mo, Mn, S and P of the sample analyzed and the standard SAE 4140 composition are shown in Tab. 4. The shaft sample is a hypoeutectoid microalloyed steel.

Table 4. Chemical composition in % weight of shaft sample and SAE 4140

|                     | C           | Si          | Cr          | Mo          | Mn          | S                    | P                    |
|---------------------|-------------|-------------|-------------|-------------|-------------|----------------------|----------------------|
| <b>Shaft Sample</b> | 0,382       | 0,245       | 0,906       | 0,189       | 0,855       | 0,028                | 0,011                |
| <b>SAE 4140</b>     | 0,37 - 0,44 | 0,15 - 0,35 | 0,75 - 1,20 | 0,15 - 0,25 | 0,65 - 1,10 | 0,030 <sub>max</sub> | 0,040 <sub>max</sub> |

### 3.2.3 Metallographic analysis

A surface of a region near the crack initiation point was metallographically prepared, etched with Nital 2% and analysed in optical microscope. Microstructure is a pearlitic matrix with ferrite in grain boundaries as shown in Fig. 8. Based on ASTM E112 the grains size is 3.

The observed microstructure is in accordance to the expected since the shaft was manufactured from a rolled round bar. According to Silva (2012), the rolling process in metal forming requires the component to be plastically deformed in one or more operations to near the net shape dimensions in order to reduce metal removal requirements resulting in significant material and energy savings during manufacturing.

Although the SAE 4140 steel is of good hardenability (Rasma, 2015), the wood chipper shaft was manufactured from a as rolled condition bar with improved machinability and appropriate mechanical properties in relation to fatigue resistance and torsion loads. As a hypoeutectoid steel in the as rolled condition, perlite is formed with low cooling rates and the microstructures at room temperature is a matrix of perlite with proeutectoid ferrite.

SAE 4140 is a chromium, molybdenum and manganese low alloy steel noted for toughness, good torsional strength and good fatigue strength (Silva, 2012). It has in its composition approximately 1% in weight of Chromium that increases wearing resistance of steels and its hardenability. Molybdenum is an alloying element in SAE 4140 composition that also increases hardenability and strength particularly at high temperatures and under dynamic conditions.

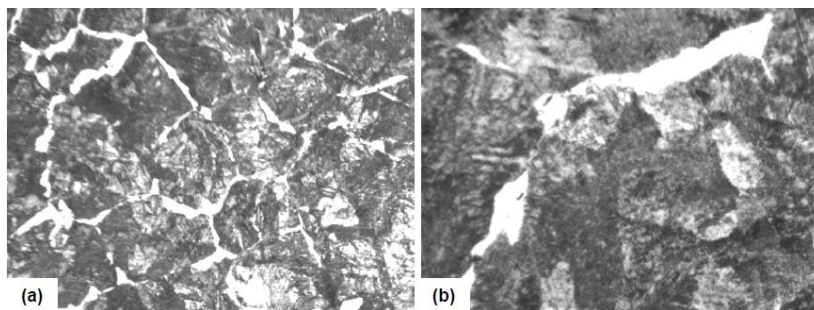


Figure 8. microstructure of pearlitic matrix with grain boundary ferrite (a) Nital 2%, 100x (b) Nital 2%, 400x

### 3.2.4 Mechanical test

The sample used for the metallographic analysis was firstly submitted to hardness testing with 0.15 and 0.30 mm depth from the shaft surface. Hardness measurements in HV and then converted to HRC are as expected related to material specification. Table 5 shows the hardness measurement results. Standard SAE 4140 hardness converted to HRC in as rolled condition is 23 to 25 (Rasma, 2015).

Table 5. Hardness measurement of the shaft sample in two levels from the surface

|              | Surface Depth (mm) | Hardness (HRC) |
|--------------|--------------------|----------------|
| Shaft Sample | 0,15               | 23,5           |
|              | 0,3                | 23,5           |

## 4. CONCLUSIONS

After investigating the fracture characteristics, it is concluded that both shafts failed due to fatigue mechanism. The fracture surface presented the topography expected of such failure mode with crack initiation, propagation and unstable crack growth that led to fracture. The crack initiation in both cases was at a concentration stress point at the surface.

The refiner shaft failure was due to crack nucleation and propagation related to torsion mechanical loads the equipment is subjected during operation. The structural deterioration initiated at a region of stress concentration that is the edge of the keyseat. Once initiated the crack, the failure followed the stages characteristic to fatigue mechanism.

Similar characteristics could be observed at the wood chipper shaft where a crack nucleated at the surface in a stress concentration point followed by a stable growth and ultimately a catastrophic failure. The investigation of the failure surface suggests that the root cause was fatigue with crack nucleation at a point of discontinuity at the shaft surface.

## 5. REFERENCES

- ASTM E1823., 1996. “Standard Terminology Relating to Fatigue and Fracture Testing”.
- Barbosa, F.E.V., 2015. *Análise das variáveis operacionais de um processo de produção de papel visando maior eficiência de operação*. M.Sc. dissertation, Universidade Estadual de Campinas, Campinas, Brasil.
- Godefroid, L.B., Faria, G.L., Cândido, L.C., Viana, T.G., 2015. “Failure analysis of recurrent cases of fatigue fracture in flash butts welded rails”. *Engineering Failure Analysis*, Vol. 58, pp. 407-416.
- IBA., 2019. “Estatística da Indústria Brasileira de Árvores - Janeiro”. 02 Mar. 2019 <<https://www.iba.org>>.
- Ihara, L.M., 2018. *Caracterização de fratura por fadiga em componentes mecânicos*. M.Sc. dissertation, Universidade de São Paulo, São Paulo, Brasil.
- Oliveira, J.A., 2017. *Fractografia quantitativa: relação entre diferentes condições de tratamento térmico e a dimensão fractal*. M.Sc. dissertation, Universidade Estadual Paulista Julio de Mesquita Filho, Guaratinguetá, Brasil.
- Rasma, E.T., 2015. *Caracterização estrutural e mecânica do aço AISI/SAE 4140 tratado sob diferentes tratamentos térmicos*. M.Sc. dissertation, Universidade Estadual do Norte Fluminense, Campos dos Goytacazes, Brasil.
- Silva, A.D., 2012. *Prediction and control of geometric distortion and residual stresses in hot rolled and heat treated large rings*. D.Sc. thesis, Universidade Federal de Minas Gerais, Belo Horizonte, Brasil.
- Sodré, R.T.M., 2008. *Avaliação da tenacidade à fratura e da resistência à fadiga de dois aços utilizados em eixos de carros torpedos*. M.Sc. dissertation, Universidade Federal de Ouro Preto, Ouro Preto, Brasil.
- SpectroScan., 2018. “Relatório de ensaios amostra 16679/2018”.
- SpectroScan., 2019. “Relatório de ensaio amostra16871/2019”.
- Voort, G.F.V., 2001. “Etching Isothermally Treated Steels”. *Heat Treating Progress*, ASM International April/May Issue.
- Zipp, R.D., Dahlberg, E.P., 1987. “Preparation and Preservation of Fracture Specimen”. *ASM Handbook*, Vol. 12: Fractography, pp. 72–77.

## 6. RESPONSIBILITY NOTICE

The author is the only responsible for the printed material included in this paper.